Natural Resources Canada
Ressources naturelles Canada

# Age dating of a bentonite in the Duo Lake Formation, western Mackenzie Mountains, Northwest Territories

*K.M. Fallas and W. Matthews*

**Geological Survey of Canada**
**Current Research 2022-2**

**2022**

Canada

Geological Survey of Canada
Current Research 2022-2

# Age dating of a bentonite in the Duo Lake Formation, western Mackenzie Mountains, Northwest Territories

*K.M. Fallas and W. Matthews*

2022

ISSN 1701-4387
ISBN 978-0-660-40119-5
Catalogue No. M44-2022/2E-PDF
https://doi.org/10.4095/328830

A copy of this publication is also available for reference in depository libraries across Canada through access to the Depository Services Program's Web site at http://dsp-psd.pwgsc.gc.ca.

This publication is available for free download through GEOSCAN (https://geoscan.nrcan.gc.ca).

**Recommended citation**

Fallas, K.M. and Matthews, W., 2022. Age dating of a bentonite in the Duo Lake Formation, western Mackenzie Mountains, Northwest Territories; Geological Survey of Canada, Current Research 2022-2, 14 p. https://doi.org/10.4095/328830

Critical review
*M.P. Cecile*

***Author(s)***

***K.M. Fallas (Karen.Fallas@nrcan-rncan.gc.ca)***
***Geological Survey of Canada***
***3303–33rd Street N.W.***
***Calgary, Alberta***
***T2L 2A7***

***W. Matthews (wamatthe@ucalgary.ca)***
***Department of Geoscience***
***University of Calgary***
***2500 University Drive N.W.***
***Calgary, Alberta***
***T2N 1N4***

Correction date:

# Age dating of a bentonite in the Duo Lake Formation, western Mackenzie Mountains, Northwest Territories

**K.M. Fallas and W. Matthews**

*Fallas, K.M. and Matthews, W., 2022. Age dating of a bentonite in the Duo Lake Formation, western Mackenzie Mountains, Northwest Territories; Geological Survey of Canada, Current Research 2022-2, 14 p. https://doi.org/10.4095/328830*

**Abstract:** In the Misty Creek Embayment of the western Mackenzie Mountains, Duo Lake Formation locally includes minor volcanic deposits associated with Marmot Formation volcanism. A bentonite layer from an outcrop of graptolitic shale found in NTS map area 106-B, in the upper part of the Duo Lake Formation, was sampled for U-Pb zircon dating. Analytical results yielded a dominant population of grains with a concordia age of 439.8 ± 3.0 Ma, interpreted as the age of deposition. Minor inherited zircon populations yielded ages ranging from approximately 1200 to 2850 Ma. Observed graptolites from the same outcrop likely range from Middle Ordovician to Early Silurian and are compatible with the interpreted U-Pb age of the bentonite. Previously known Middle and Late Ordovician volcanic activity in the Misty Creek Embayment is here expanded to include Early Silurian activity, and serves as a proxy for the timing of active extensional tectonism in the basin.

**Résumé :** Dans le rentrant de Misty Creek, dans la partie ouest des monts Mackenzie, la Formation de Duo Lake renferme par endroits une quantité mineure de dépôts volcaniques associés au volcanisme de la Formation de Marmot. Dans un affleurement de shale graptolitique repéré dans la région cartographique 106-B du SNRC, nous avons échantillonné une couche de bentonite située dans la partie supérieure de la Formation de Duo Lake aux fins de datation U-Pb sur zircon. Les résultats d'analyse ont révélé une population dominante de grains livrant un âge concordia de 439,8 ± 3,0 Ma, interprété comme étant l'âge du dépôt. Des populations mineures de zircons hérités ont livré des âges variant entre 2850 et 1200 Ma environ. Les graptolites observés dans le même affleurement datent probablement de l'Ordovicien moyen au Silurien précoce, ce qui concorde avec l'âge U-Pb interprété de la bentonite. L'activité volcanique déjà connue dans le rentrant de Misty Creek remontant à l'Ordovicien moyen et tardif est ici étendue pour englober l'activité datant du Silurien précoce et sert d'indicateur indirect pour déterminer quand une tectonique de distension s'est manifestée dans le bassin.

Corresponding author: K.M. Fallas (Karen.Fallas@nrcan-rncan.gc.ca)

## INTRODUCTION

Volcanic deposits in Cambrian to Devonian strata are documented in the Canadian Cordilleran miogeocline from southeastern British Columbia to the Northwest Territories and Yukon (Goodfellow et al., 1995). These alkalic and ultrapotassic deposits are typically found as isolated volcanic piles and spatially restricted thin beds and lenses in shale-dominated basinal strata deposited on the former western edge of the North American margin (i.e. Laurentian margin). While relative dating of these deposits using fossil constraints in associated strata is often possible (e.g. Taylor et al., 1972; McArthur et al., 1980; Cecile, 1982; Hart, 1986; Norford and Cecile, 1994), direct radiometric dating (e.g. Godwin and Price, 1986; Leslie, 2009; MacNaughton et al., 2016) is less common.

An outcrop of graptolitic shale of the Duo Lake Formation, with interbedded layers of bentonite, was found within NTS map area 106-B in part of the Misty Creek Embayment (Cecile, 1982), of the western Mackenzie Mountains (Fig. 1). Sampling bentonite from this outcrop provided an opportunity to attempt U-Pb age dating of zircon in volcanic deposits from a stratigraphic unit that previously lacked direct radiometric dating, and compare to age assignments based on graptolite fauna. This paper reports on the radiometric dating of one bentonite layer and discusses the implications for the record of volcanic activity in the Misty Creek Embayment.

## GEOLOGICAL SETTING AND BACKGROUND

The Misty Creek Embayment was a semi-enclosed basin of deep-water deposition lying between the Mackenzie and Ogilvie platforms, and opening toward present-day south into the Selwyn Basin across the Niddery High (Fig. 1). Cecile (1982) described the embayment as extensional in

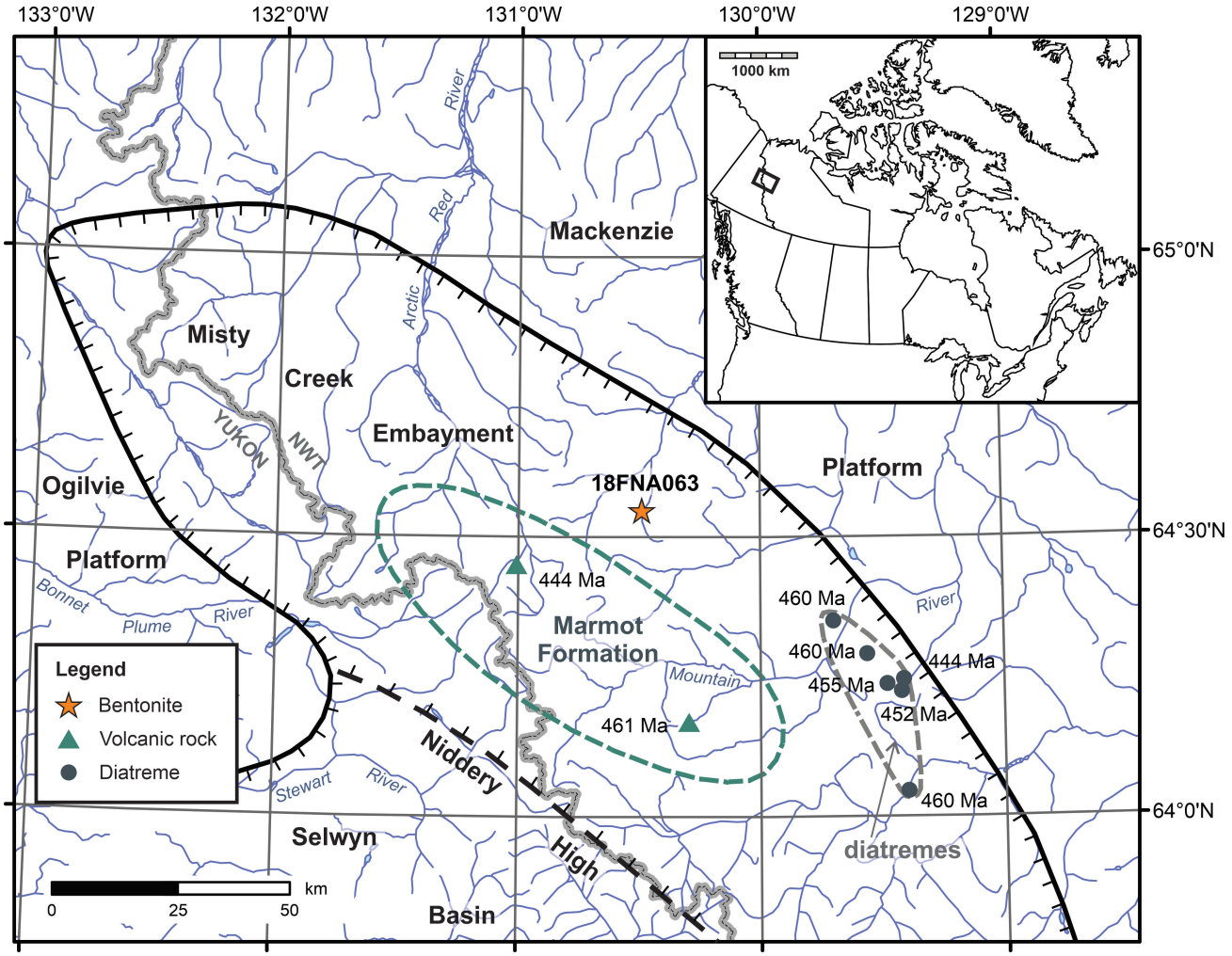


**Figure 1.** Location of study area in western Mackenzie Mountains, inset shows location within Canada. Ordovician-Silurian limit of the Misty Creek Embayment (black line with ticks), mapped extent of Marmot Formation (green dashed line), and extent of diatremes (grey dashed line) shown for context. Sampled bentonite location marked with orange star (this study). Dated diatremes and Marmot Formation volcanic rocks from Leslie (2009).

origin and compared it to a segment of the East African Rift system. The basin was a paleogeographic feature from Cambrian to Silurian time with dominantly shale and deep-water carbonate deposition (Cecile, 1982). Within the Misty Creek Embayment, Cecile (1982) documented extension-related volcanic deposits of the Marmot Formation in strata spanning the Middle Ordovician to Early Silurian (Fig. 2), interleaved with strata of the Duo Lake and Cloudy formations. Cecile (1982) also documented volcanic deposits in Late Silurian to Early or middle Devonian strata, which were originally included in the Marmot Formation and later treated as a separate, unnamed volcanic package (Goodfellow et al., 1995). Mappable thicknesses of Marmot Formation are limited to the middle of the Misty Creek Embayment, where the unit varies from 0 to 500 m thick (Cecile, 1982). Elsewhere in the basin, minor beds of volcanic material can be found within Duo Lake and Cloudy formations. One set of Middle to Late Ordovician Ar-Ar dates for volcanic deposits of the Marmot Formation and related diatremes within the Misty Creek Embayment range from 460 to 444 Ma (Leslie, 2009). Cecile et al. (1997, their Figure 3) interpreted the Misty Creek Embayment to have had two distinct rift cycles — one with rifting commencing in late Early Cambrian to Middle Cambrian, and the other with rifting commencing in the Middle Ordovician — the Marmot Formation volcanic deposits were considered a product of the Ordovician rift event.

Just south of the Misty Creek Embayment, in the Selwyn Basin, are additional scattered thick successions of lower Paleozoic volcanic rocks ranging in age from Cambrian to Silurian and known as the Old Cabin Formation (Cecile 2000, Hart, 1986). At the Old Cabin Creek massif, Hart (1986) described one of these occurrences as a 500 m thick succession of hyaloclastic breccias with lesser amounts of massive flows, pillowed flows, lapilli tuffs, epiclastics, and associated sills and dykes. Here the Old Cabin Formation overlies and crosscuts Late Cambrian argillite, and is overlain by a graptolitic unit of earliest Silurian age. Subsequent biostratigraphic studies combined with U-Pb

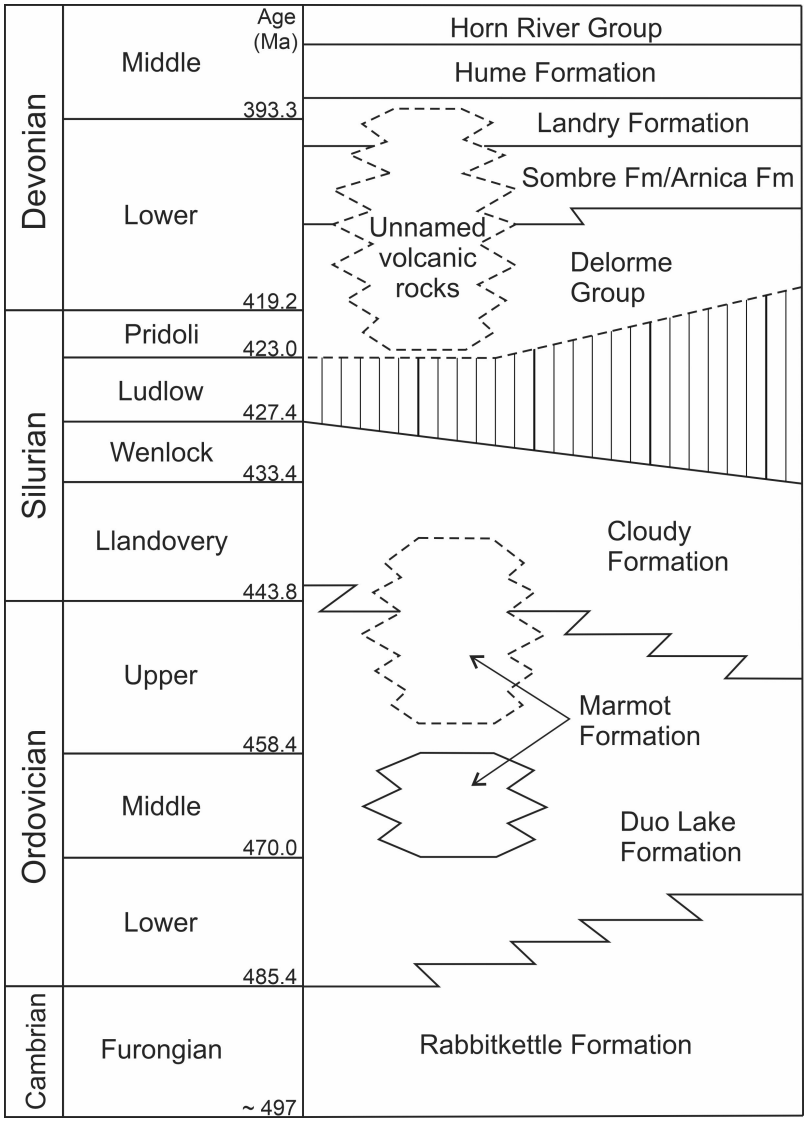


**Figure 2.** Stratigraphic relationships within the Misty Creek Embayment from centre (left side) to northeast margin (right side) of the basin. Vertical hatching indicates a gap in the stratigraphic record, and dashed lines indicate less precise age constraints on unit boundaries.

dating of zircons from volcaniclastic sandstone of the Old Cabin Formation led MacNaughton et al. (2016) to restrict the Old Cabin Formation to Cambrian volcanic deposits. These relationships emphasize the need to better understand the possible links between extension-related volcanism in the Misty Creek Embayment and similar volcanism in the Selwyn Basin.

Located within the Misty Creek Embayment, station 18FNA063 (Fig. 1) is an outcrop of interbedded graptolitic shale, bentonite, and minor lime mudstone (Fig. 3). The graptolitic shale is black, thinly-laminated, fissile, and is the dominant lithology in the outcrop. An attempt was made to sample graptolites from this shale for detailed study, but the attempt was unsuccessful due to the fissile nature of the shale. The bentonite is green-grey on fresh surfaces and rusty on weathered surfaces, it occurs as beds 1–3 cm thick, and is soft and crumbly. Minor lime mudstone beds are dark grey, laminated, and range from 1–15 cm thick. This outcrop is interpreted as Duo Lake Formation due to the predominance of shale, the limited volume of volcanic material, and its position beyond the extent of mappable Marmot Formation. However, the bentonite layers in this outcrop are likely related to Marmot Formation volcanism.

## METHODS

Two layers of bentonite observed at station 18FNA063 (64°32′44.0″N, 130°29′17.5″W, NAD83) were collected for zircons (Fig. 3a, b). These samples were subsequently processed for zircons and analyzed at the Calgary Geo- and Thermochronology Lab of the University of Calgary. Detrital zircons were separated using standard mineral separation techniques of crushing, milling, water tabling, heavy liquids and magnetic separation. Due to the small size of the sample and the resultant low-zircon yield, all of the zircon-rich separate was dump-mounted into a 12 × 15 mm Teflon™ form and cast in epoxy. Mounts were ground using 5 µm SiC film adhered to glass. Grinding continued until the surface reached roughly the midpoint of the smallest zircon population in the mount. Initial polishing employed 3 diamond-abrasive film adhered to glass. A final polish was performed using Struers 1 µm Dia-Duo2™ diamond paste on a MD-Dur™ polishing cloth. This polishing procedure ensured that all zircon populations in the sample were available for measurement and provided a very flat finish to ensure consistent laser focus.

Prior to measurement, grains were cathodoluminescence (CL) imaged to investigate internal textures. Imaging was performed using a FEITM Quanta™ 250 FEG scanning electron microscope equipped with a Gatan™ MonoCL4 Elite CL detection and imaging instrument. CL images were used to select ablation locations.

U-Pb isotopic data were collected by laser-ablation inductively coupled plasma mass spectrometry (LA-ICP-MS). Ablation occurred in a Laurin Technic™ M-50 two-volume ablation cell in an Applied Spectra Resolution 193 nm laser ablation system. Samples were ablated for 35 seconds using a 22 µm beam diameter, a fluence of 2.1 J/cm$^2$, and a repetition rate of 7 Hz. A signal-smoothing manifold (Squid) was used to smooth out rapid changes in isotopic signal intensity (beating) which could occur at lower repetition rates (Müller et al., 2009). Each ablation was proceeded by a 20-second gas blank. These laser settings resulted in a ~22 µm deep pit. Additional information and performance metrics for the laser-ablation system can be found in Müller et al. (2009). Isotopic signal intensities were measured using an Agilent 7700x quadrupole mass spectrometer.

Samples were measured using a sample-standard bracketing procedure. One measurement of the calibration reference material (FC1; 1099.9 Ma; Paces and Miller, 1993) was made between each four to five unknowns (approximately every 7 minutes). Eight measurements of SRM-NIST610 glass were used to calibrate U and Th concentrations. Zirconium was used to standardize these concentrations and assumed stoichiometric abundance (49.7 wt %). Eight measurements of each of five validation reference materials (Table 1) were used to validate the results. A total of 66 unknowns were measured.

Data were reduced using the commercially available Iolite™ (V2.5; Paton et al., 2010) software package and the VizualAge data reduction scheme (Petrus and Kamber, 2012). Time-resolved age, U/Th ratios, and isotopic signal intensities were checked for each measurement to identify issues such as Pb-loss, common Pb, age heterogeneities or measurements where the ablation pit exited the grain during measurement. Integration periods were modified to exclude regions of grains affected by these problems.

Uncertainty propagation was performed in a custom Excel™ VBA macro (ARS5.0) in accordance with community-derived best practices outlined in Horstwood et al. (2016) using the method of Matthews and Guest (2017). Standard deviations of the mean ($s_m$) were calculated as the standard deviation of all the indications of the isotopic ratio in the integration period, divided by the square root of the number of indications. Excess variance (ε) in the $^{206}Pb/^{238}U$ and $^{207}Pb/^{206}Pb$ ratios was calculated using an intrasessional approach as outlined in Matthews and Guest (2017) and added quadratically to $s_m$ to give the random data point uncertainty ($s_x$). Long-term excess variance (ε′) was calculated using excess variance in validation reference materials 91500 ($^{206}Pb/^{238}U$; 1.2%) and 1242 ($^{207}Pb/^{206}Pb$; 0.7%). Systematic uncertainties associated with decay constants (λ), uncertainty in the ratios of the calibration reference material ($s_y$), and ε′ were added in quadrature to yield the total uncertainty ($s_{total}$).

Data were filtered using the probability of concordance calculated by the concordia age algorithm in Isoplot 4.15 (Ludwig, 1998; Ludwig, 2012). Measurements with <1% probability of concordance were filtered from the data set. Probability density functions were generated in DZStats


**Figure 3.** Photos of outcrop 18FNA063: **a)** view looking west showing positions of graptolites and sampled bentonite layer, photograph by K.M. Fallas, NRCan photo 2021–124; **b)** closer view of slightly rusty bentonite layers with the sampled layer indicated by white arrow, where hammer handle is approximately 30 cm long, photograph by K.M. Fallas, NRCan photo 2021–123; **c)** graptolites on shale bedding plane. Graptolite marked with arrow shows better preserved detail of thecae. Photograph by K.M. Fallas. NRCan photo 2021–122

**Table 1.** Information pertaining to the calibration and validation reference materials used.

| Reference material | Geological unit | Age (Ma) | | Reference |
|---|---|---|---|---|
| | | $^{206}Pb/^{238}U$ | $^{207}Pb/^{206}Pb$ | |
| FCT | Fish Canyon Tuff | 28.201 ± 0.046 | N/A | Kuiper et al. (2008) |
| Temora 2 | Middledale gabbroic complex | 416.78 ± 0.33 | N/A | Black et al. (2004) |
| 91500 | Kuehl Lake, Ontario | 1062.4 ± 0.4 | 1065.4 ± 0.3 | Wiedenbeck et al. (1995, 2004) |
| FC-1 | Duluth Anorthosite | 1099.9 ± 1.1 | 1099.0 ± 0.6 | Paces and Miller (1993) |
| 1242 | Lac Frechette Syenite | 2675.1 ± 1.1 | 2679.8 ± 0.2 | Mortensen and Card (1993); Davis et al. (2019) |

(Saylor and Sundell, 2016) and have been plotted using $^{206}Pb/^{238}U$ dates for grains younger than 1500 Ma and $^{207}Pb/^{206}Pb$ dates for grains older than 1500 Ma. All sources of random and systematic uncertainty were included in the plots. A concordia age (Ludwig, 1998) was calculated for the near-depositional-age grain populations using IsoplotR (Vermeesch, 2018).

## RESULTS

Only one of the two bentonite samples yielded zircons (18FNA063C02). Zircon grains from this sample were generally colourless, short, simple prismatic morphologies (2:1 aspect ratio) or fragments of prismatic grains. The grains show no evidence of significant transport in a sedimentary system (abrasion). Cathodoluminescence imaging reveals mostly low to moderate luminescence oscillatory zoning (Fig. 4). Some grains exhibit discordant zoning in the core of the grain that may represent inherited cores, although these were not systematically targeted to test this observation. The observed zoning and low U/Th ratios for these grains (average of 1.4) are consistent with growth from a magma (Corfu et al., 2003).

Sample 18FNA063C02 (lab ID 102–2) yielded 66 zircon grains that were datable and 61 grains yielded concordant results (Table 2). The vast majority of grains yielded latest Ordovician to Early Silurian dates, with a mode in the probability density plot at ~441 Ma (Fig. 5A). There are minor grain populations at approximately 2550–2850 Ma, 1900–2100 Ma, and 1200 Ma. A weighted average of all the grains <1.0 Ga yielded a $^{206}Pb/^{238}U$ age of 440 Ma with an MSWD of 2.7, which suggests that they are not a single population. A concordia age for the youngest population is likely the most precise measure of the population's age (Ludwig, 1998; Spencer et al., 2016; Vermeesch, 2018) and yields 439.8 ± 3.0 Ma from 53 grains (Fig. 5B). This is the best estimate of the maximum depositional age. The concordia age calculation also resulted in a low probability of equivalence for the measurements suggesting there is more dispersion in the dates than would be expected given the analytical uncertainties (MSWD of equivalence was 1.9). This means either the uncertainties were underestimated, or there is more than one population present in the near-depositional age grains. Given that the sample is a bentonite and there is a limited number of older detrital grains, the latter is unlikely.

## DISCUSSION

Biostratigraphic age constraints for the Duo Lake Formation, based mainly on graptolite collections, indicate an age range of Early Ordovician to Early Silurian (Cecile, 1982). Much of the unit yields fauna with tighter age ranges in either the Early or Middle Ordovician, but some sections include longer ranging fauna spanning the Middle Ordovician to Early Silurian (see Section 9 of Cecile, 1982). As a result, the age limit of the upper contact of the Duo Lake Formation may be as old as Middle Ordovician or as young as Early Silurian. In many cases, the age of volcanic deposits of the Marmot Formation are based on fossil collections in units below and above, and in a few cases, fossil debris within the volcanic deposits. Based on these data, Marmot Formation volcanic deposits appear in Middle Ordovician, Late Ordovician to Early Silurian, and possibly Early Devonian strata (Cecile, 1982). Previous Ar-Ar dating of phlogopite in Marmot Formation volcanic rocks has yielded two dates of 460.6 ± 2.6 Ma and 444.5 ± 2.6 Ma (Leslie, 2009), verifying the Middle and Late Ordovician volcanic activity during deposition of the Duo Lake Formation.

Sample 18FNA063C02 was collected along strike 20 km to the southeast from published measured sections by Cecile (1982; Section 6) and Morrow (1991; Section 21), within the same structural panel. By tracing unit boundaries along strike from the measured sections, the sampled outcrop appears to lie in the upper part of the Duo Lake Formation (Fig. 6). The integrated biostratigraphic data from the nearby sections suggests this interval of the Duo Lake Formation may be Middle Ordovician to Early Silurian based on graptolites, and Late Ordovician to Early Silurian based on conodonts (Cecile, 1982). The interpreted age of 439.8 ± 3.0 Ma from this study indicates an Early Silurian depositional age for the bentonite, and is therefore compatible with the younger age limit of the Duo Lake Formation from regional biostratigraphic data. It is also worth noting that the interpreted age of the bentonite is not compatible

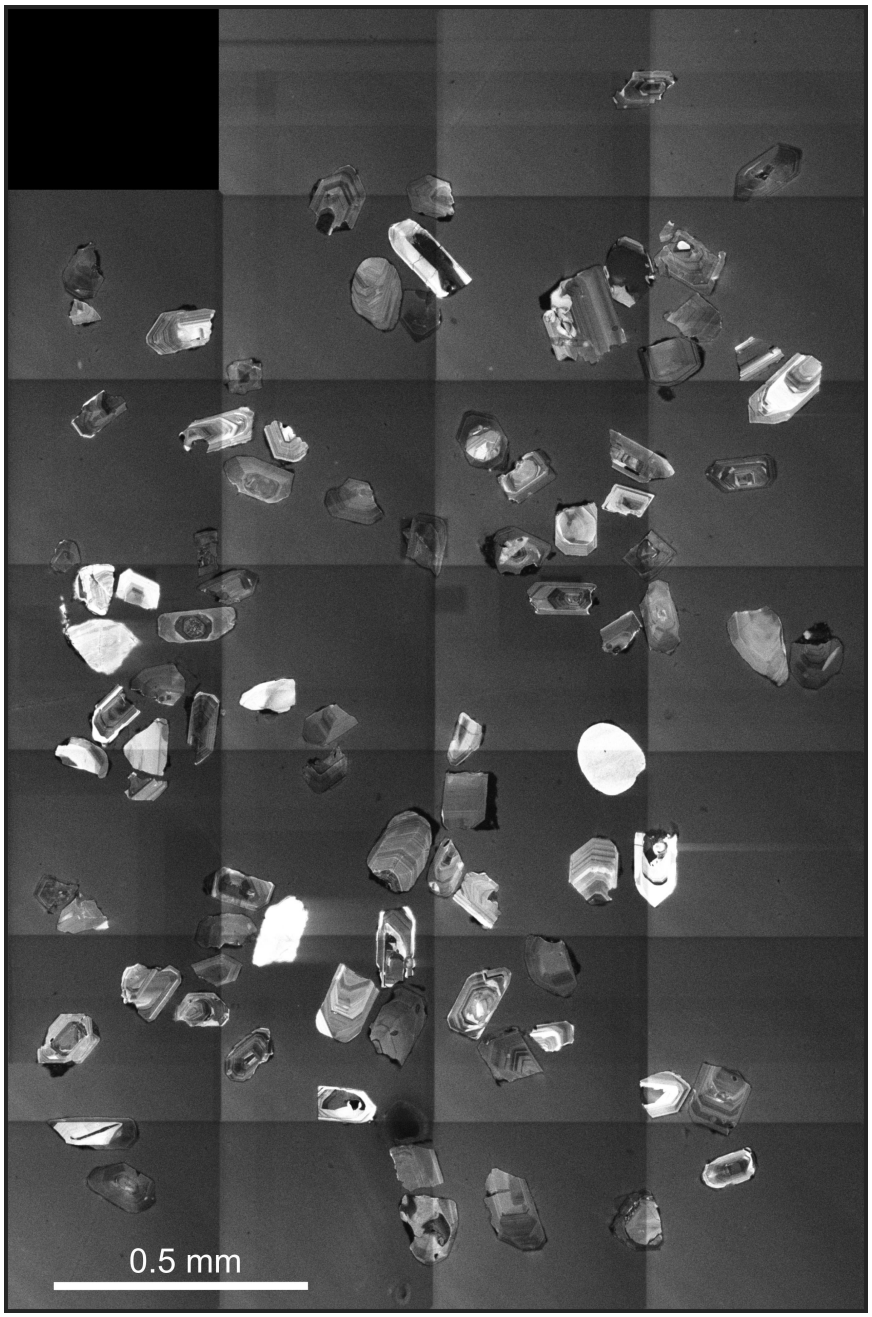


**Figure 4.** Cathodoluminescence images of zircon from sample 18FN063C02.

with Middle Ordovician graptolites reported from this interval of Duo Lake Formation at Section 6 of Cecile (1982), and may be an indication there are errors in the correlation of strata between Section 6 and the sampled outcrop.

The graptolites observed approximately 1 m below the sampled bentonite in the outcrop (Fig. 3c) may also be compatible with an Early Silurian age. These are a biserial diplograptid type, similar to late Middle Ordovician to Early Silurian genera previously documented from the Selwyn Basin and Misty Creek Embayment (Lenz, 1979, 1982; B.S. Norford in Cecile, 1982; Berry, 1996). Varied Early Ordovician graptolite forms collected from the lower part of the Duo Lake Formation (Jackson and Norford, 2004; Jackson and Lenz, 2006) are typically branching forms that differ markedly from those illustrated in Figure 3. This also supports the interpretation that the sampled outcrop lies within the upper part of the Duo Lake Formation.

Along with the analyzed zircon grains that yielded a Paleozoic age, there are eight accepted grain ages in excess of 1000 Ma. It is likely that these grains were incorporated either into the magma from country rock preceding eruption, or into the volcanic ash during eruption. If so, these grains are likely derived from pre-Ordovician strata underlying the Mackenzie Mountains. Potential sources for these grains include Neoproterozoic sandstone units found in the Katherine Group, Rapitan Group, and Keele Formation,

**Table 2.** U-Pb isotopic analytical data for zircon grains from sample 18FNA063C02.

| University of Calgary | | | | Validation reference | FCT | TRD | Temora | 91500 | FC1 | 1242 | | | | | | | | | | | | | | | | | | | |
|---|---|---|---|---|---|---|---|---|---|---|---|---|---|---|---|---|---|---|---|---|---|---|---|---|---|---|---|---|---|
| Calgary Geo- and Thermochronology Lab | | | | $^{206}Pb/^{238}U$ (Ma) | 28.2 | 61.2 | 416.7 | 1062.4 | 1099.9 | 2672.4 | | | | | | | | | | | | | | | | | | | |
| Session | 20210322_VT112_KF102 | | | $\Delta^{206}Pb/^{238}U$ Age (%) | -6.1 | | -1.7 | -2.6 | 0.0 | 0.0 | | | | | | | | | | | | | | | | | | | |
| Date | 22/03/2021 | | | $\Delta^{207}Pb/^{206}Pb$ Age (%) | | | | -0.5 | 0.4 | -0.8 | | | | | | | | | | | | | | | | | | | |
| | | | | | | Data for Tera-Wasserburg plot[2] | | | | Data for Wetherill plot[2] | | | | | Dates | | | | | | | | | Prob. conc. (%) | % conc[3] | Comments | Accepted dates | | |
| Sample | Spot | $^{207}Pb$ CPS | $^{206}Pb$ CPS | U (ppm)[1] | U/Th | $^{238}U/^{206}Pb$ | $2s_x$ (%) | $^{207}Pb/^{206}Pb$ | $2s_x$ (%) | $^{207}Pb/^{235}Pb$ | $2s_x$ (%) | $^{206}Pb/^{238}U$ | $2s_x$ (%) | Rho | $^{207}Pb/^{206}Pb$ | $2s_x$ (ABS) | $2s_{total}$ (ABS) | $^{206}Pb/^{238}U$ | $2s_x$ (ABS) | $2s_{total}$ (ABS) | $^{207}Pb/^{235}Pb$ | $2s_x$ (ABS) | $2s_{total}$ (ABS) | | | | Date (Ma) | $2s_x$ (ABS) | $2s_{total}$ (ABS) |
| 102-2 | UK102_2_11 | 115.7 | 2080 | 432.4 | 0.8 | 14.7710 | 2.9 | 0.0536 | 8.0 | 0.50033 | 8.5 | 0.06770 | 2.9 | 0.06 | NA | NA | NA | 422.3 | 11.8 | 13.0 | 411.9 | 28.7 | 29.1 | 49.4 | NA | | 422.3 | 11.8 | 13.0 |
| 102-2 | UK102_2_17 | 253 | 4510 | 997 | 1.7 | 14.7493 | 2.2 | 0.0543 | 5.9 | 0.50761 | 6.4 | 0.06780 | 2.2 | 0.30 | NA | NA | NA | 422.9 | 9.2 | 10.7 | 416.8 | 21.7 | 22.2 | 56.3 | NA | CL, LL | 422.9 | 9.2 | 10.7 |
| 102-2 | UK102_2_2 | 88.8 | 1578 | 331.4 | 1.2 | 14.7059 | 3.2 | 0.0539 | 9.1 | 0.50536 | 9.6 | 0.06800 | 3.2 | 0.12 | NA | NA | NA | 424.1 | 13.2 | 14.3 | 415.3 | 32.8 | 33.1 | 60.2 | NA | | 424.1 | 13.2 | 14.3 |
| 102-2 | UK102_2_7 | 315 | 5350 | 964 | 1.0 | 14.7059 | 2.2 | 0.0579 | 5.3 | 0.54286 | 5.7 | 0.06800 | 2.2 | 0.28 | NA | NA | NA | 424.1 | 9.1 | 10.6 | 440.3 | 20.4 | 21.0 | 10.6 | NA | DO | 424.1 | 9.1 | 10.6 |
| 102-2 | UK102_2_31 | 83.2 | 1460 | 281.2 | 1.0 | 14.6628 | 3.3 | 0.0540 | 9.1 | 0.50778 | 9.7 | 0.06820 | 3.3 | 0.05 | NA | NA | NA | 425.3 | 13.5 | 14.6 | 417.0 | 33.3 | 33.6 | 63.5 | NA | | 425.3 | 13.5 | 14.6 |
| 102-2 | UK102_2_46 | 80.5 | 1275 | 297.4 | 1.2 | 14.6413 | 3.5 | 0.0616 | 9.7 | 0.58010 | 10.3 | 0.06830 | 3.5 | -0.08 | NA | NA | NA | 425.9 | 14.4 | 15.5 | 464.5 | 38.3 | 38.7 | 7.0 | NA | | 425.9 | 14.4 | 15.5 |
| 102-2 | UK102_2_21 | 120 | 2157 | 394.8 | 1.6 | 14.4928 | 2.9 | 0.0521 | 8.1 | 0.49566 | 8.6 | 0.06900 | 2.9 | 0.12 | NA | NA | NA | 430.1 | 12.2 | 13.4 | 408.8 | 29.1 | 29.4 | 15.4 | NA | LL, DO | 430.1 | 12.2 | 13.4 |
| 102-2 | UK102_2_61 | 242 | 4490 | 856 | 1.4 | 14.4928 | 2.2 | 0.0543 | 5.6 | 0.51659 | 6.0 | 0.06900 | 2.2 | 0.25 | NA | NA | NA | 430.1 | 9.1 | 10.7 | 422.9 | 20.8 | 21.4 | 47.9 | NA | | 430.1 | 9.1 | 10.7 |
| 102-2 | UK102_2_13 | 157 | 2560 | 524.1 | 1.3 | 14.4300 | 2.7 | 0.0571 | 6.9 | 0.54560 | 7.4 | 0.06930 | 2.7 | 0.05 | NA | NA | NA | 431.9 | 11.1 | 12.5 | 442.1 | 26.6 | 27.1 | 47.4 | NA | | 431.9 | 11.1 | 12.5 |
| 102-2 | UK102_2_26 | 347 | 6010 | 1062 | 0.9 | 14.4300 | 2.0 | 0.0552 | 4.9 | 0.52744 | 5.3 | 0.06930 | 2.0 | -0.07 | NA | NA | NA | 431.9 | 8.5 | 10.2 | 430.1 | 18.5 | 19.1 | 86.1 | NA | CL | 431.9 | 8.5 | 10.2 |
| 102-2 | UK102_2_12 | 72.1 | 1294 | 221 | 1.3 | 14.3678 | 3.7 | 0.0547 | 10.2 | 0.52493 | 10.9 | 0.06960 | 3.7 | 0.28 | NA | NA | NA | 433.7 | 15.6 | 16.6 | 428.4 | 37.9 | 38.2 | 77.2 | NA | LL | 433.7 | 15.6 | 16.6 |
| 102-2 | UK102_2_63 | 116.8 | 1925 | 369.2 | 1.3 | 14.3678 | 3.0 | 0.0591 | 7.9 | 0.56715 | 8.5 | 0.06960 | 3.0 | 0.07 | NA | NA | NA | 433.7 | 12.5 | 13.8 | 456.2 | 31.2 | 31.6 | 17.5 | NA | | 433.7 | 12.5 | 13.8 |
| 102-2 | UK102_2_32 | 144 | 2521 | 459.5 | 1.5 | 14.3472 | 2.7 | 0.0544 | 7.1 | 0.52280 | 7.7 | 0.06970 | 2.7 | 0.10 | NA | NA | NA | 434.3 | 11.5 | 12.8 | 427.0 | 26.7 | 27.1 | 59.9 | NA | | 434.3 | 11.5 | 12.8 |
| 102-2 | UK102_2_14 | 134.2 | 2389 | 486.1 | 1.3 | 14.3266 | 2.8 | 0.0536 | 7.5 | 0.51585 | 8.0 | 0.06980 | 2.8 | 0.14 | NA | NA | NA | 435.0 | 11.7 | 13.0 | 422.4 | 27.7 | 28.1 | 37.5 | NA | | 435.0 | 11.7 | 13.0 |
| 102-2 | UK102_2_48 | 203 | 3510 | 723 | 1.4 | 14.3266 | 2.4 | 0.0539 | 6.1 | 0.51873 | 6.5 | 0.06980 | 2.4 | 0.06 | NA | NA | NA | 435.0 | 10.0 | 11.5 | 424.3 | 22.7 | 23.1 | 37.8 | NA | | 435.0 | 10.0 | 11.5 |
| 102-2 | UK102_2_33 | 183 | 3240 | 592 | 1.5 | 14.3062 | 2.4 | 0.0536 | 6.4 | 0.51659 | 6.9 | 0.06990 | 2.4 | 0.00 | NA | NA | NA | 435.6 | 10.2 | 11.7 | 422.9 | 23.7 | 24.2 | 32.4 | NA | | 435.6 | 10.2 | 11.7 |
| 102-2 | UK102_2_53 | 94.7 | 1633 | 331.8 | 1.4 | 14.3062 | 3.2 | 0.0546 | 8.7 | 0.52622 | 9.3 | 0.06990 | 3.2 | 0.24 | NA | NA | NA | 435.6 | 13.4 | 14.6 | 429.3 | 32.5 | 32.8 | 69.6 | NA | | 435.6 | 13.4 | 14.6 |
| 102-2 | UK102_2_16 | 126.8 | 2110 | 429.2 | 1.4 | 14.2857 | 2.8 | 0.0573 | 7.5 | 0.55304 | 8.0 | 0.07000 | 2.8 | 0.09 | NA | NA | NA | 436.2 | 11.9 | 13.2 | 447.0 | 29.1 | 29.5 | 47.9 | NA | | 436.2 | 11.9 | 13.2 |
| 102-2 | UK102_2_25 | 128.9 | 2123 | 409 | 1.5 | 14.2653 | 2.8 | 0.0570 | 7.5 | 0.55093 | 8.1 | 0.07010 | 2.8 | 0.06 | NA | NA | NA | 436.8 | 12.0 | 13.3 | 445.6 | 29.1 | 29.5 | 56.6 | NA | | 436.8 | 12.0 | 13.3 |
| 102-2 | UK102_2_51 | 150 | 2730 | 513.8 | 1.2 | 14.2653 | 2.7 | 0.0538 | 7.0 | 0.52000 | 7.5 | 0.07010 | 2.7 | 0.12 | NA | NA | NA | 436.8 | 11.6 | 12.9 | 425.1 | 26.2 | 26.6 | 39.3 | NA | DO | 436.8 | 11.6 | 12.9 |
| 102-2 | UK102_2_39 | 246 | 3910 | 807 | 1.0 | 14.2450 | 2.3 | 0.0591 | 5.6 | 0.57204 | 6.0 | 0.07020 | 2.3 | 0.03 | NA | NA | NA | 437.4 | 9.8 | 11.4 | 459.3 | 22.3 | 22.9 | 7.1 | NA | | 437.4 | 9.8 | 11.4 |
| 102-2 | UK102_2_60 | 231 | 3980 | 569 | 1.1 | 14.2450 | 2.6 | 0.0551 | 6.4 | 0.53332 | 6.9 | 0.07020 | 2.6 | 0.13 | NA | NA | NA | 437.4 | 10.8 | 12.2 | 434.0 | 24.3 | 24.8 | 79.1 | NA | DO | 437.4 | 10.8 | 12.2 |
| 102-2 | UK102_2_54 | 199 | 3220 | 671.1 | 1.6 | 14.2248 | 2.5 | 0.0573 | 6.2 | 0.55541 | 6.6 | 0.07030 | 2.5 | 0.03 | NA | NA | NA | 438.0 | 10.4 | 11.9 | 448.5 | 24.1 | 24.6 | 41.7 | NA | | 438.0 | 10.4 | 11.9 |
| 102-2 | UK102_2_1 | 328 | 5530 | 1000 | 1.6 | 14.2045 | 2.1 | 0.0545 | 5.4 | 0.52902 | 5.8 | 0.07040 | 2.1 | 0.05 | NA | NA | NA | 438.6 | 8.9 | 10.6 | 431.2 | 20.3 | 20.8 | 49.6 | NA | DO | 438.6 | 8.9 | 10.6 |
| 102-2 | UK102_2_42 | 179 | 3010 | 617 | 1.8 | 14.1844 | 2.5 | 0.0566 | 6.6 | 0.55018 | 7.1 | 0.07050 | 2.5 | 0.11 | NA | NA | NA | 439.2 | 10.8 | 12.2 | 445.1 | 25.4 | 25.9 | 65.5 | NA | | 439.2 | 10.8 | 12.2 |
| 102-2 | UK102_2_66 | 153 | 2580 | 417 | 1.3 | 14.1844 | 2.7 | 0.0560 | 7.2 | 0.54435 | 7.7 | 0.07050 | 2.7 | -0.09 | NA | NA | NA | 439.2 | 11.5 | 12.9 | 441.3 | 27.6 | 28.1 | 89.1 | NA | LL | 439.2 | 11.5 | 12.9 |
| 102-2 | UK102_2_3 | 229 | 4170 | 783 | 1.5 | 14.1643 | 2.2 | 0.0545 | 5.8 | 0.53052 | 6.2 | 0.07060 | 2.2 | 0.21 | NA | NA | NA | 439.8 | 9.4 | 11.0 | 432.2 | 21.9 | 22.4 | 48.6 | NA | | 439.8 | 9.4 | 11.0 |
| 102-2 | UK102_2_23 | 126.8 | 2090 | 367.1 | 1.4 | 14.1243 | 2.9 | 0.0599 | 7.5 | 0.58474 | 8.0 | 0.07080 | 2.9 | 0.34 | NA | NA | NA | 441.0 | 12.3 | 13.6 | 467.5 | 30.1 | 30.5 | 6.5 | NA | | 441.0 | 12.3 | 13.6 |
| 102-2 | UK102_2_40 | 431 | 6570 | 1128 | 1.2 | 14.1243 | 2.0 | 0.0599 | 4.5 | 0.58474 | 4.9 | 0.07080 | 2.0 | -0.01 | NA | NA | NA | 441.0 | 8.6 | 10.3 | 467.5 | 18.5 | 19.1 | 1.0 | NA | DO | 441.0 | 8.6 | 10.3 |
| 102-2 | UK102_2_24 | 65.3 | 1148 | 211 | 1.6 | 14.0845 | 3.6 | 0.0529 | 10.2 | 0.51786 | 10.8 | 0.07100 | 3.6 | 0.01 | NA | NA | NA | 442.2 | 15.2 | 16.3 | 423.7 | 37.5 | 37.8 | 35.5 | NA | | 442.2 | 15.2 | 16.3 |
| 102-2 | UK102_2_57 | 309 | 5290 | 1126 | 1.2 | 14.0845 | 2.1 | 0.0553 | 5.0 | 0.54136 | 5.4 | 0.07100 | 2.1 | 0.19 | NA | NA | NA | 442.2 | 8.8 | 10.6 | 439.3 | 19.4 | 20.0 | 77.2 | NA | | 442.2 | 8.8 | 10.6 |
| 102-2 | UK102_2_5 | 207 | 3720 | 655 | 1.4 | 14.0647 | 2.4 | 0.0542 | 6.2 | 0.53134 | 6.7 | 0.07110 | 2.4 | 0.15 | NA | NA | NA | 442.8 | 10.3 | 11.8 | 432.7 | 23.5 | 24.0 | 40.5 | NA | DO | 442.8 | 10.3 | 11.8 |
| 102-2 | UK102_2_36 | 112 | 1854 | 292.7 | 1.3 | 14.0647 | 3.1 | 0.0561 | 8.4 | 0.54996 | 8.9 | 0.07110 | 3.1 | 0.05 | NA | NA | NA | 442.8 | 13.4 | 14.6 | 445.0 | 32.2 | 32.5 | 89.8 | NA | DO | 442.8 | 13.4 | 14.6 |
| 102-2 | UK102_2_6 | 121 | 2070 | 422.4 | 1.4 | 14.0252 | 3.0 | 0.0554 | 7.9 | 0.54463 | 8.4 | 0.07130 | 3.0 | -0.02 | NA | NA | NA | 444.0 | 12.8 | 14.0 | 441.5 | 30.3 | 30.6 | 87.9 | NA | | 444.0 | 12.8 | 14.0 |
| 102-2 | UK102_2_58 | 147 | 2500 | 511.3 | 1.2 | 14.0056 | 2.7 | 0.0553 | 7.2 | 0.54441 | 7.7 | 0.07140 | 2.7 | 0.09 | NA | NA | NA | 444.6 | 11.6 | 13.0 | 441.3 | 27.5 | 27.9 | 82.1 | NA | | 444.6 | 11.6 | 13.0 |
| 102-2 | UK102_2_19 | 153 | 2630 | 430 | 1.6 | 13.9860 | 2.8 | 0.0567 | 7.6 | 0.55897 | 8.1 | 0.07150 | 2.8 | 0.08 | NA | NA | NA | 445.2 | 12.0 | 13.3 | 450.9 | 29.3 | 29.8 | 71.4 | NA | CL, LL | 445.2 | 12.0 | 13.3 |
| 102-2 | UK102_2_22 | 302 | 5150 | 1026 | 1.5 | 13.9860 | 2.1 | 0.0553 | 5.1 | 0.54517 | 5.5 | 0.07150 | 2.1 | 0.24 | NA | NA | NA | 445.2 | 9.0 | 10.7 | 441.8 | 19.7 | 20.3 | 73.1 | NA | | 445.2 | 9.0 | 10.7 |

**Table 2. (cont.)** U-Pb isotopic analytical data for zircon grains from sample 18FNA063C02.

| University of Calgary | | | | Validation reference | FCT | TRD | Temora | 91500 | FC1 | 1242 | | | | | | | | | | | | | | | | | | |
|---|---|---|---|---|---|---|---|---|---|---|---|---|---|---|---|---|---|---|---|---|---|---|---|---|---|---|---|---|
| Calgary Geo- and Thermochronology Lab | | | | $^{206}Pb/^{238}U$ (Ma) | 28.2 | 61.2 | 416.7 | 1062.4 | 1099.9 | 2672.4 | | | | | | | | | | | | | | | | | | |
| Session | 20210322_VT112_KF102 | | | $\Delta^{206}Pb/^{238}U$ Age (%) | -6.1 | | -1.7 | -2.6 | 0.0 | 0.0 | | | | | | | | | | | | | | | | | | |
| Date | 22/03/2021 | | | $\Delta^{207}Pb/^{206}Pb$ Age (%) | | | | -0.5 | 0.4 | -0.8 | | | | | | | | | | | | | | | | | | |
| | | | | | | Data for Tera-Wasserburg plot[2] | | | | Data for Wetherill plot[2] | | | | | Dates | | | | | | | | | | | Accepted dates | | |
| Sample | Spot | $^{207}Pb$ CPS | $^{206}Pb$ CPS | U (ppm)[1] | U/Th | $^{238}U/^{206}Pb$ | $2s_x$ (%) | $^{207}Pb/^{206}Pb$ | $2s_x$ (%) | $^{207}Pb/^{235}Pb$ | $2s_x$ (%) | $^{206}Pb/^{238}U$ | $2s_x$ (%) | Rho | $^{207}Pb/^{206}Pb$ | $2s_x$ (ABS) | $2s_{total}$ (ABS) | $^{206}Pb/^{238}U$ | $2s_x$ (ABS) | $2s_{total}$ (ABS) | $^{207}Pb/^{235}Pb$ | $2s_x$ (ABS) | $2s_{total}$ (ABS) | Prob. conc. (%) | % conc[3] | Comments | Date (Ma) | $2s_x$ (ABS) | $2s_{total}$ (ABS) |
| 102-2 | UK102_2_62 | 208 | 3540 | 687.1 | 1.5 | 13.9860 | 2.4 | 0.0557 | 6.1 | 0.54911 | 6.5 | 0.07150 | 2.4 | 0.04 | NA | NA | NA | 445.2 | 10.2 | 11.7 | 444.4 | 23.4 | 23.9 | 95.1 | NA | | 445.2 | 10.2 | 11.7 |
| 102-2 | UK102_2_43 | 151.1 | 2522 | 543 | 1.7 | 13.9665 | 2.6 | 0.0562 | 7.0 | 0.55482 | 7.5 | 0.07160 | 2.6 | 0.19 | NA | NA | NA | 445.8 | 11.4 | 12.8 | 448.1 | 27.2 | 27.6 | 86.4 | NA | | 445.8 | 11.4 | 12.8 |
| 102-2 | UK102_2_50 | 260 | 4450 | 826 | 1.3 | 13.9665 | 2.2 | 0.0570 | 5.5 | 0.56272 | 5.9 | 0.07160 | 2.2 | 0.16 | NA | NA | NA | 445.8 | 9.4 | 11.0 | 453.3 | 21.5 | 22.0 | 49.6 | NA | | 445.8 | 9.4 | 11.0 |
| 102-2 | UK102_2_44 | 87.1 | 1411 | 311.5 | 1.1 | 13.9276 | 3.4 | 0.0588 | 9.1 | 0.58211 | 9.7 | 0.07180 | 3.4 | 0.09 | NA | NA | NA | 447.0 | 14.6 | 15.7 | 465.8 | 36.3 | 36.7 | 32.5 | NA | | 447.0 | 14.6 | 15.7 |
| 102-2 | UK102_2_47 | 27.1 | 444 | 93.1 | 1.4 | 13.9276 | 5.2 | 0.0610 | 16.0 | 0.60389 | 16.8 | 0.07180 | 5.2 | -0.18 | NA | NA | NA | 447.0 | 22.4 | 23.2 | 479.7 | 64.2 | 64.4 | 36.7 | NA | | 447.0 | 22.4 | 23.2 |
| 102-2 | UK102_2_4 | 266 | 4830 | 860 | 1.4 | 13.9082 | 2.2 | 0.0530 | 5.7 | 0.52542 | 6.1 | 0.07190 | 2.2 | 0.09 | NA | NA | NA | 447.6 | 9.4 | 11.1 | 428.8 | 21.3 | 21.9 | 9.3 | NA | DO | 447.6 | 9.4 | 11.1 |
| 102-2 | UK102_2_15 | 207 | 3539 | 641 | 1.6 | 13.8889 | 2.4 | 0.0565 | 6.1 | 0.56090 | 6.6 | 0.07200 | 2.4 | 0.07 | NA | NA | NA | 448.2 | 10.4 | 12.0 | 452.1 | 23.9 | 24.4 | 75.8 | NA | | 448.2 | 10.4 | 12.0 |
| 102-2 | UK102_2_10 | 222 | 4000 | 819 | 1.4 | 13.8696 | 2.2 | 0.0529 | 5.9 | 0.52589 | 6.3 | 0.07210 | 2.2 | 0.10 | NA | NA | NA | 448.8 | 9.7 | 11.4 | 429.1 | 22.0 | 22.5 | 8.6 | NA | | 448.8 | 9.7 | 11.4 |
| 102-2 | UK102_2_37 | 330 | 5830 | 919 | 1.0 | 13.8504 | 2.7 | 0.0533 | 6.6 | 0.53060 | 7.1 | 0.07220 | 2.7 | -0.33 | NA | NA | NA | 449.4 | 11.7 | 13.1 | 432.2 | 25.1 | 25.6 | 26.6 | NA | DO | 449.4 | 11.7 | 13.1 |
| 102-2 | UK102_2_18 | 297 | 4990 | 903 | 1.7 | 13.8313 | 2.1 | 0.0580 | 5.1 | 0.57819 | 5.5 | 0.07230 | 2.1 | 0.01 | NA | NA | NA | 450.0 | 9.0 | 10.8 | 463.3 | 20.5 | 21.1 | 23.6 | NA | | 450.0 | 9.0 | 10.8 |
| 102-2 | UK102_2_52 | 275 | 4463 | 790 | 1.6 | 13.8313 | 2.2 | 0.0571 | 5.4 | 0.56921 | 5.8 | 0.07230 | 2.2 | 0.11 | NA | NA | NA | 450.0 | 9.4 | 11.1 | 457.5 | 21.5 | 22.1 | 50.6 | NA | | 450.0 | 9.4 | 11.1 |
| 102-2 | UK102_2_65 | 271 | 4680 | 872 | 1.5 | 13.8313 | 2.2 | 0.0558 | 5.5 | 0.55625 | 5.9 | 0.07230 | 2.2 | 0.07 | NA | NA | NA | 450.0 | 9.4 | 11.1 | 449.1 | 21.4 | 21.9 | 93.6 | NA | | 450.0 | 9.4 | 11.1 |
| 102-2 | UK102_2_8 | 182 | 3180 | 646 | 1.2 | 13.7552 | 2.5 | 0.0568 | 6.5 | 0.56936 | 7.0 | 0.07270 | 2.5 | 0.08 | NA | NA | NA | 452.4 | 10.7 | 12.3 | 457.6 | 25.6 | 26.1 | 70.1 | NA | | 452.4 | 10.7 | 12.3 |
| 102-2 | UK102_2_49 | 60.5 | 1166 | 239.4 | 1.0 | 13.6426 | 3.6 | 0.0498 | 10.7 | 0.50331 | 11.2 | 0.07330 | 3.6 | 0.11 | NA | NA | NA | 456.0 | 15.7 | 16.8 | 413.9 | 38.2 | 38.5 | 3.2 | NA | | 456.0 | 15.7 | 16.8 |
| 102-2 | UK102_2_64 | 211 | 3570 | 622 | 1.7 | 13.5870 | 2.4 | 0.0545 | 6.2 | 0.55306 | 6.7 | 0.07360 | 2.4 | -0.03 | NA | NA | NA | 457.8 | 10.6 | 12.2 | 447.0 | 24.1 | 24.6 | 41.6 | NA | | 457.8 | 10.6 | 12.2 |
| 102-2 | UK102_2_55 | 45.4 | 847 | 133.5 | 1.0 | 13.0039 | 4.4 | 0.0515 | 12.8 | 0.54605 | 13.5 | 0.07690 | 4.4 | 0.05 | NA | NA | NA | 477.6 | 20.2 | 21.1 | 442.4 | 48.5 | 48.8 | 16.8 | NA | CL | 477.6 | 20.2 | 21.1 |
| 102-2 | UK102_2_41 | 235 | 2570 | 177.1 | 2.9 | 4.8948 | 2.7 | 0.0852 | 5.8 | 2.39999 | 6.4 | 0.20430 | 2.7 | 0.11 | 1320.1 | 112.5 | 116.4 | 1198.4 | 29.9 | 33.4 | 1242.6 | 45.9 | 47.0 | 9.3 | 9.2 | | 1198.4 | 29.9 | 33.4 |
| 102-2 | UK102_2_20 | 836 | 6620 | 242.8 | 1.2 | 2.8694 | 2.0 | 0.1186 | 3.2 | 5.69887 | 3.8 | 0.34850 | 2.0 | 0.35 | 1935.2 | 57.8 | 64.1 | 1927.4 | 32.9 | 39.9 | 1931.2 | 32.7 | 34.7 | 84.1 | 0.4 | LL | 1935.2 | 57.8 | 64.1 |
| 102-2 | UK102_2_34 | 349 | 2741 | 95.8 | 1.2 | 2.7548 | 2.7 | 0.1191 | 4.9 | 5.96101 | 5.6 | 0.36300 | 2.7 | 0.31 | 1942.8 | 87.0 | 91.3 | 1996.4 | 47.1 | 52.5 | 1970.2 | 48.6 | 50.0 | 35.0 | -2.8 | | 1942.8 | 87.0 | 91.3 |
| 102-2 | UK102_2_45 | 183 | 1400 | 61.4 | 1.2 | 2.8653 | 3.4 | 0.1237 | 6.4 | 5.95246 | 7.3 | 0.34900 | 3.4 | 0.17 | 2010.3 | 114.2 | 117.5 | 1929.8 | 56.7 | 61.0 | 1968.9 | 63.3 | 64.4 | 31.5 | 4.0 | | 2010.3 | 114.2 | 117.5 |
| 102-2 | UK102_2_35 | 980 | 7410 | 188.8 | 1.9 | 2.5974 | 2.3 | 0.1263 | 3.9 | 6.70448 | 4.5 | 0.38500 | 2.3 | 0.32 | 2047.1 | 69.7 | 74.8 | 2099.6 | 40.8 | 47.4 | 2073.2 | 40.2 | 42.0 | 26.3 | -2.6 | DO | 2047.1 | 69.7 | 74.8 |
| 102-2 | UK102_2_9 | 630 | 3480 | 109.3 | 2.0 | 2.1459 | 2.4 | 0.1731 | 3.7 | 11.12204 | 4.5 | 0.46600 | 2.4 | 0.33 | 2587.8 | 62.4 | 67.5 | 2466.0 | 49.9 | 57.1 | 2533.4 | 41.6 | 43.4 | 1.2 | 4.7 | | 2587.8 | 62.4 | 67.5 |
| 102-2 | UK102_2_38 | 393 | 1920 | 43 | 1.6 | 1.8519 | 3.8 | 0.1880 | 4.8 | 13.99758 | 6.2 | 0.54000 | 3.8 | 0.49 | 2724.7 | 79.9 | 83.9 | 2783.4 | 86.8 | 92.0 | 2749.5 | 58.7 | 60.0 | 38.3 | -2.2 | DO | 2724.7 | 79.9 | 83.9 |
| 102-2 | UK102_2_56 | 2040 | 9650 | 213.3 | 2.5 | 1.7668 | 1.9 | 0.2020 | 2.3 | 15.76410 | 3.0 | 0.56600 | 1.9 | 0.50 | 2842.4 | 37.7 | 45.4 | 2891.4 | 43.2 | 53.5 | 2862.6 | 28.3 | 31.1 | 13.5 | -1.7 | LL | 2842.4 | 37.7 | 45.4 |
| 102-2 | UK102_2_27 | 370 | 1520 | 540 | 1.5 | 9.5238 | 14.3 | 0.2220 | 16.9 | 3.21398 | 22.1 | 0.10500 | 14.3 | 1.00 | 2995.3 | 274.7 | 275.8 | 643.6 | 87.6 | 88.0 | 1460.5 | 173.0 | 173.3 | 0.0 | 78.5 | DO | | | |
| 102-2 | UK102_2_28 | 407 | 5010 | 1626 | 1.9 | 13.3333 | 2.6 | 0.0780 | 4.8 | 0.80660 | 5.4 | 0.07500 | 2.6 | -0.03 | NA | NA | NA | 466.2 | 11.6 | 13.1 | 600.5 | 24.6 | 25.4 | 0.0 | NA | | | | |
| 102-2 | ~~UK102_2_29~~ | ~~234~~ | ~~3520~~ | ~~854~~ | ~~1.4~~ | ~~14.1844~~ | ~~2.5~~ | 0.0639 | 6.1 | 0.62114 | 6.6 | 0.07050 | 2.5 | 0.22 | NA | NA | NA | 439.2 | 10.7 | 12.1 | 490.6 | 25.7 | 26.2 | 0.0 | NA | DO, E | | | |
| 102-2 | UK102_2_30 | 334 | 3080 | 149.7 | 1.1 | 3.8625 | 2.5 | 0.1032 | 5.0 | 3.68394 | 5.6 | 0.25890 | 2.5 | 0.23 | 1682.5 | 91.6 | 96.0 | 1484.2 | 33.3 | 37.8 | 1567.9 | 44.4 | 45.7 | 0.1 | 11.8 | | | | |
| 102-2 | UK102_2_59 | 314 | 5140 | 1185 | 1.0 | 15.3139 | 2.3 | 0.0611 | 5.5 | 0.55012 | 6.0 | 0.06530 | 2.3 | 0.22 | NA | NA | NA | 407.8 | 9.1 | 10.5 | 445.1 | 21.5 | 22.0 | 0.1 | NA | | | | |

[1]Concentration uncertainty 5%
[2]Data not corrected for common lead
[3]Concordance calculated as ($^{206}Pb/^{238}U$ age/$^{207}Pb$-$^{206}Pb$ age)*100
[4]Accepted dates have probability of concordance >1%
Decay constants of Jaffey et al. (1971) used with modification after Mattinson (1987)
NA = not available
$s_x$ includes all random uncertainties ($s_m$, ε); $s_{total}$ includes all random and systematic uncertainties ($s_m$, ε, ε′, $s_y$, λ)
Comments: CL - analysis affected by common Pb; DO - pit drilled out of grain; LL - affected by lead loss; E - analysis is not sound, eliminated

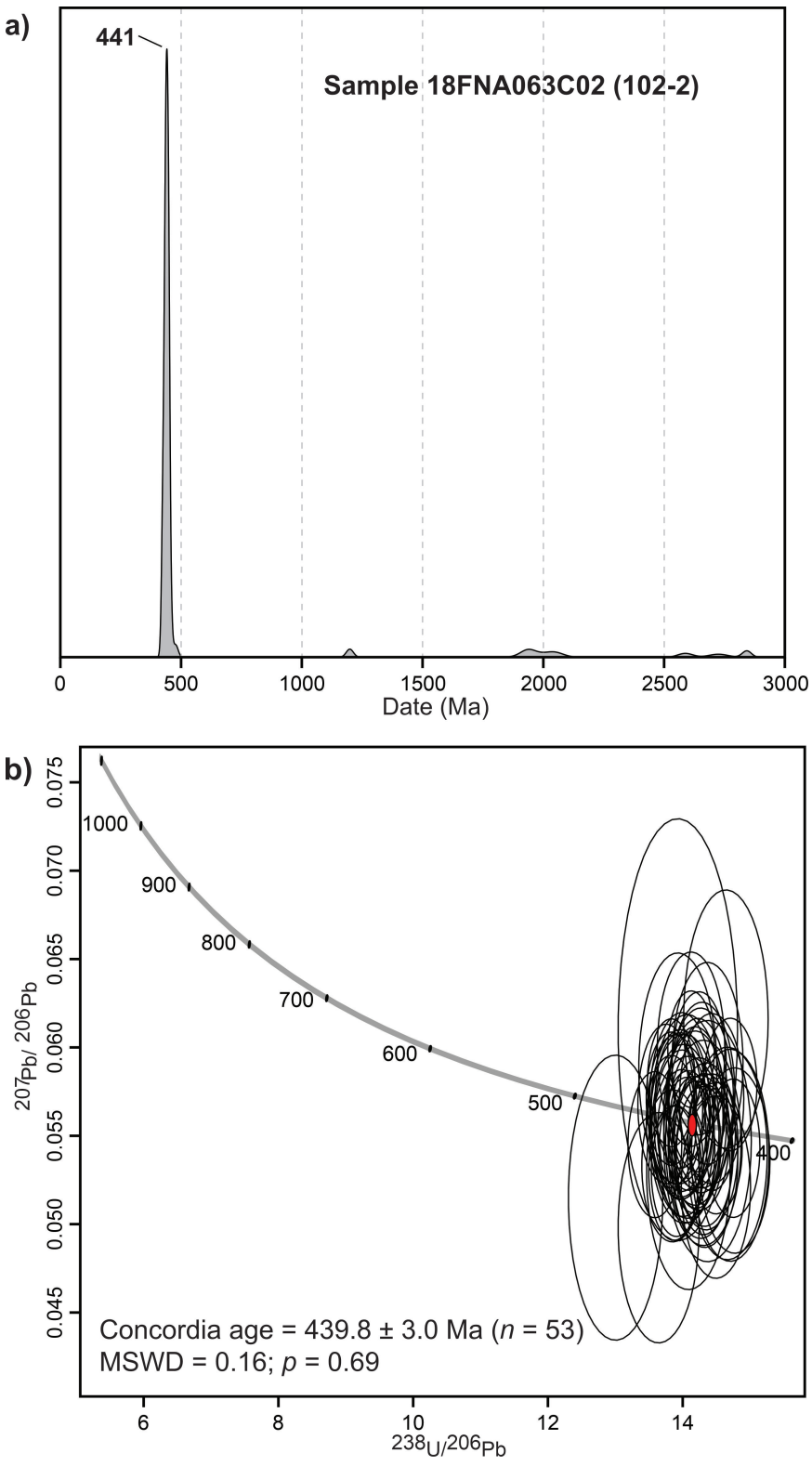


**Figure 5.** Results of U-Pb dating of zircon grains from sample 18FNA063C02: **a)** probability density function for grain ages showing dominant population mode at 441 Ma; **b)** Tera–Wasserburg concordia diagram of Paleozoic grains showing a cluster of concordant ages and concordia age (red ellipse) illustrating the best estimate eruptive age of the bentonite.

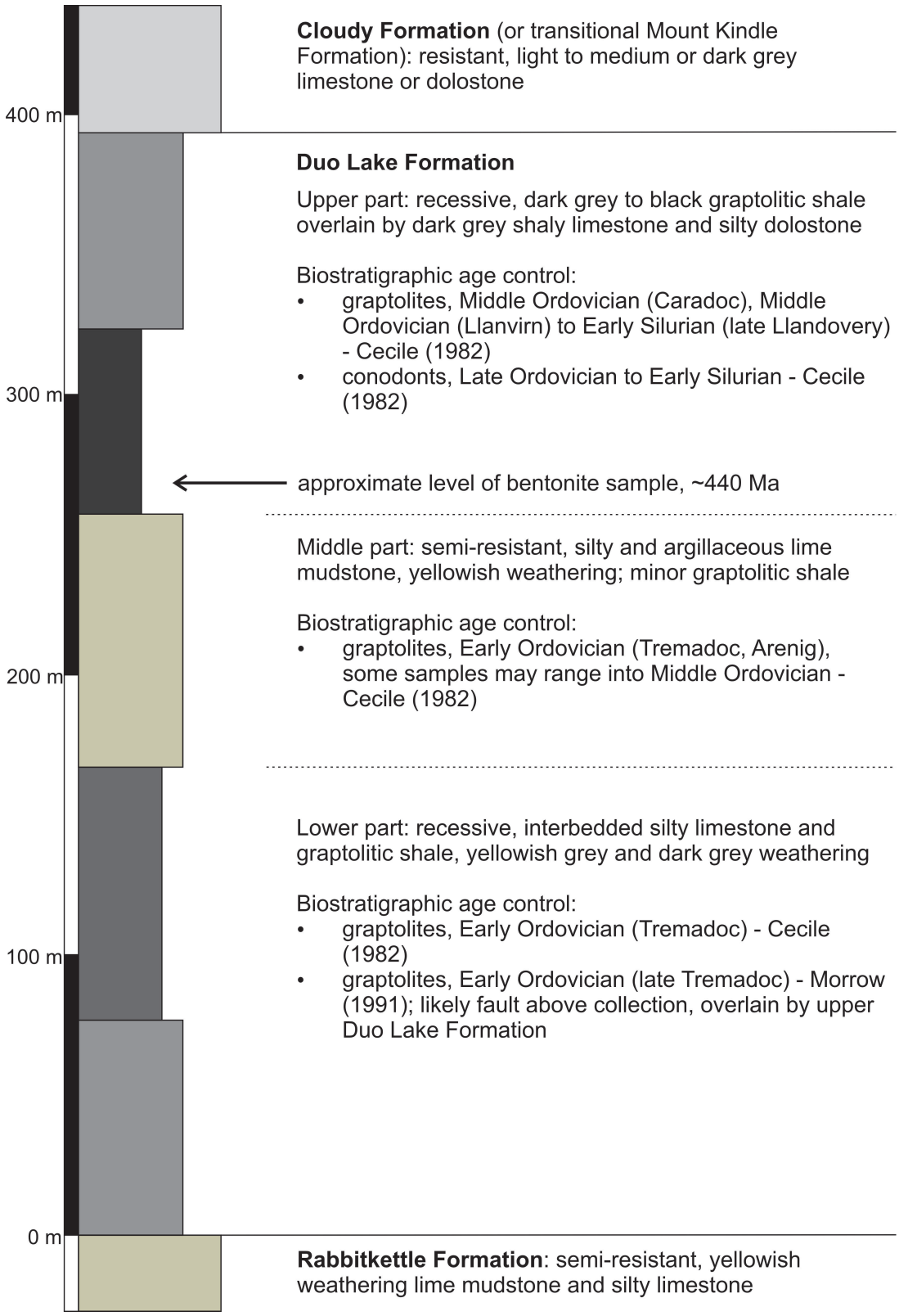


**Figure 6.** Duo Lake stratigraphy and biostratigraphic data near outcrop 18FNA063. Composite stratigraphic column and fossil information based on measured section 6 of Cecile (1982) and section 21 of Morrow (1991), modified by mapping observations. Colours reflect weathering colour of interval, whereas the width of the interval reflects the weathering profile. Reinterpreted upper contact of Duo Lake Formation is placed ~60 m higher than contact of Cecile (1982).

Neoproterozoic to Cambrian Backbone Ranges Formation, or other undocumented Proterozoic units in the subsurface. Of the older grain populations found in this study, grains around 1200 Ma are found in the Katherine Group, Rapitan Group, and Keele Formation (Lane and Gehrels, 2014; Rainbird et al., 2017). Grains in the 1900–2100 Ma range are found in the Rapitan Group, Keele Formation, and Backbone Ranges Formation (Leslie, 2009; Lane and Gehrels, 2014). Archean grains in the 2550–2850 Ma range are a minor component in the Katherine Group, Rapitan Group, and Keele Formation (Lane and Gehrels, 2014; Rainbird et al., 2017), but are a larger component of the Backbone Ranges Formation (Leslie, 2009).

Diatremes from the central Mackenzie Mountains have been chemically linked to Marmot Formation volcanic deposits (Goodfellow et al., 1995). Initial radiometric dates for these diatremes include latest Ordovician to Silurian K-Ar dates (whole-rock and phlogopite) of 445 ± 17 Ma and 424 ± 15 Ma for the Mountain and Bear diatremes respectively (Godwin and Price, 1986), suggesting the diatremes are somewhat younger than the Marmot Formation. More recent and more precise Ar-Ar dating on phlogopite by Leslie (2009) has yielded dates of 451.9 ± 2.6 Ma (Late Ordovician) for the Mountain diatreme, and 459.9 ± 2.5 Ma (Middle Ordovician) for the Bear diatreme. In addition, Leslie (2009) reports Ar-Ar dates for four other diatremes ranging from 444.4 ± 2.5 Ma to 459.7 ± 2.5 Ma. These data demonstrate diatreme emplacement overlapped with Marmot Formation volcanic activity during the Middle and Late Ordovician in the Misty Creek Embayment. The close association between Duo Lake Formation and volcanic strata of the Marmot Formation explains the local presence of bentonite layers in Duo Lake Formation, and the depositional age of ~440 Ma for the bentonite reported here indicates volcanic activity associated with the Marmot Formation continued into the Early Silurian.

## CONCLUSIONS

Graptolite collections from the Duo Lake Formation indicate the strata range from late Early Ordovician to likely as young as Early Silurian. Existing Ar-Ar dates for Marmot Formation volcanic deposits interleaved with Duo Lake Formation verify Middle and Late Ordovician ages for these strata. The new U-Pb date based on zircon grains from a bentonite in the Duo Lake Formation support the interpretation that the upper part of the Duo Lake Formation may be as young as Early Silurian. This age is also consistent with graptolites from the same outcrop that may range from Middle Ordovician to Early Silurian, and with regional biostratigraphic data. The resulting implication is that episodic volcanic activity within the Misty Creek Embayment, and any associated extensional tectonism, ranged from Middle Ordovician to Early Silurian.

## ACKNOWLEDGMENTS

This work was conducted as part of the Mackenzie Project (2015–2020) of the Geo-mapping for Energy and Minerals (GEM) program of the Geological Survey of Canada. Thanks are extended to L. Komaromi for assistance in the field, to J. Blake-McLeod for wildlife monitor services, to Sahtu Helicopters for safe and reliable transportation in the Mackenzie Mountains, and to Scott Tiede for his help in the laboratory components of this work. Thank you to M.P. Cecile for a constructive review of this paper.

## REFERENCES

Berry, W.B.N., 1996. Recovery of post-Late Ordovician extinction graptolites: a western North American perspective; *in* Biotic Recovery from Mass Extinction Events, (ed.) M.B. Hart; Geological Society Special Publication 102, p. 119–126. https://doi.org/10.1144/GSL.SP.1996.001.01.09

Black, L.P., Kamo, S.L., Allen, C.M., Davis, D.W., Aleinkoff, J.N., Valley, J.W., Mundil, R., Campbell, I.H., Korsch, R.J., Williams, I.S., and Foudoulis, C., 2004. Improved $^{206}Pb/^{238}U$ microprobe geochronology by the monitoring of trace-element-related matrix effects; SHRIMP, ID-TIMS, ELA-ICP-MS and oxygen isotope documentation for a series of zircon standards; Chemical Geology, v. 205, p. 115–140. https://doi.org/10.1016/j.chemgeo.2004.01.003

Cecile, M.P., 1982. The lower Paleozoic Misty Creek Embayment, Selwyn Basin, Yukon and Northwest Territories; Geological Survey of Canada, Bulletin 335, 78 p. https://doi.org/10.4095/111346

Cecile, M.P., 2000. Geology of the northeastern Niddery Lake map area, east-central Yukon and adjacent Northwest Territories; Geological Survey of Canada, Bulletin 553, 120 p. https://doi.org/10.4095/211664

Cecile, M.P., Morrow, D.W., and Williams, G.K., 1997. Early Paleozoic (Cambrian to Early Devonian) tectonic framework, Canadian Cordillera; Bulletin of Canadian Petroleum Geology, v. 45, p. 54–74. https://doi.org/10.35767/gscpgbull.45.1.054

Corfu, F., Hanchar, J.M., Hosking, P.W.O., and Kinny, P., 2003. Atlas of zircon textures; Reviews in Mineralogy and Geochemistry, v. 53, p. 469–500. https://doi.org/10.2113/0530469

Davis, W.J., Pestaj, T., Rayner, N., and McNicoll, V.M., 2019. Long-term reproducibility of $^{207}Pb/^{206}Pb$ age at the GSC SHRIMP lab based on the GSC Archean reference zircon z1242; Geological Survey of Canada, Scientific Presentations 111, 1 poster. https://doi.org/10.4095/321203

Godwin, C.I. and Price, B.J., 1986. Geology of the Mountain diatreme kimberlite, north-central Mackenzie Mountains, District of Mackenzie, Northwest Territories; *in* Mineral Deposits of the Northern Cordillera, J.A. Morin (ed.); Canadian Institute of Mining and Metallurgy, Special Volume 37, p. 298–310.

Goodfellow, W.D., Cecile, M.P., and Leybourne, M.I., 1995. Geochemistry, petrogenesis, and tectonic setting of lower Paleozoic alkalic and potassic volcanic rocks, Northern Canadian Cordilleran Miogeocline; Canadian Journal of Earth Sciences, v. 32, p. 1236–1254. https://doi.org/10.1139/e95-101

Hart, C.J.R., 1986. The geology of the Old Cabin Massif, Selwyn Basin, Yukon Territory; BSc thesis, McMaster University, Hamilton, Ontario, Canada, 111 p. https://macsphere.mcmaster.ca/handle/11375/12093

Horstwood, M.S.A., Košler, J., Gehrels, G., Jackson, S.E., McLean, N.M., Paton, C., Pearson, N.J., Sircombe, K., Sylvester, P., Vermeesch, P., Bowring, J.F., Condon, D.J., and Schoene, B., 2016. Community-derived standards for LA-ICP-MS U-Th-Pb geochronology — uncertainty propagation, age interpretation and data reporting; Geostandards and Geoanalytical Research, v. 40, p. 311–332. https://doi.org/10.1111/j.1751-908X.2016.00379.x

Jackson, D.E. and Lenz, A.C., 2006. The sequence and correlation of Early Ordovician (Arenig) graptolite faunas in the Richardson Trough and Misty Creek Embayment, Yukon Territory and District of Mackenzie, Canada; Canadian Journal of Earth Sciences, v. 43, p. 1791–1820. https://doi.org/10.1139/e06-065

Jackson, D.E. and Norford, B.S., 2004. Biostratigraphical and ecostratigraphical significance of Tremadoc (Ordovician) graptolite faunas from the Misty Creek Embayment and Selwyn Basin in Yukon and Northwest Territories; Canadian Journal of Earth Sciences, v. 41, p. 331–348. https://doi.org/10.1139/e04-007

Jaffey, A.H., Flynn, K.F., Glendenin, L.E., Bentley, W.C., and Essling, A.M., 1971. Precision measurement of half-lives and specific activities of $^{235}$U and $^{238}$U; Physical Review C, v. 4, p. 1889–1906. https://doi.org/10.1103/PhysRevC.4.1889

Kuiper, K.F., Deino, A., Hilgen, F.J., Krijgsman, W., Renne, P.R., and Wijbrans, J.R., 2008. Synchronizing rock clocks of Earth history; Science, v. 320, p. 500–504. https://doi.org/10.1126/science.1154339

Lane, L.S. and Gehrels, G.E., 2014. Detrital zircon lineages of Late Neoproterozoic and Cambrian strata, NW Laurentia; Geological Society of America Bulletin, v. 126, p. 398–414. https://doi.org/10.1130/B30848.1

Lenz, A.C., 1979. Llandoverian graptolite zonation in the northern Canadian Cordillera; Acta Palaeontologica Polonica, v. 24, p. 137–153. https://www.app.pan.pl/article/item/app24-137.html

Lenz, A.C., 1982. Llandoverian graptolites of the northern Canadian Cordillera: *Petalograptus*, *Cephalograptus*, *Rhaphidograptus*, *Dimorphograptus*, Retiolitidae, and Monograptidae; Life Sciences Contributions, Royal Ontario Museum, 130, 154 p. https://doi.org/10.5962/bhl.title.60100

Leslie, C.D., 2009. Detrital zircon geochronology and rift-related magmatism: central Mackenzie Mountains, Northwest Territories. M.Sc. thesis, University of British Columbia, Vancouver, British Columbia, Canada, 224 p. https://doi.org/10.14288/1.0052744

Ludwig, K.R., 1998. On the treatment of concordant uranium-lead ages; Geochimica et Cosmochimica Acta, v. 62, p. 665–676. https://doi.org/10.1016/S0016-7037(98)00059-3

Ludwig, K.R., 2012. Isoplot v. 3.75 — A geochronological toolkit for Microsoft Excel; Berkeley Geochronology Center, Special Publication, **5**, p. 1–75.

MacNaughton, R.B., Moynihan, D.P., Roots, C.F., and Crowley, J.L., 2016. New occurrences of *Oldhamia i*n eastern Yukon, Canada: stratigraphic context and implications for Cambrian deep-marine biostratigraphy; Ichnos, v. 23, p. 33–52. https://doi.org/10.1080/10420940.2015.1127232

Matthews, W.A. and Guest, B., 2017. A practical approach to collecting large-*n* detrital zircon U-Pb data sets by quadrupole LA-ICP-MS; Geostandards and Geoanalytical Research, v. 41, p. 161–180. https://doi.org/10.1111/ggr.12146

Mattinson, J.M., 1987. U-Pb ages of zircons: A basic examination of error propagation; Chemical Geology, v. 66, p. 151–162. https://doi.org/10.1016/0168-9622(87)90037-6

McArthur, M.L., Tipnis, R.S., and Godwin, C.I., 1980. Early and Middle Ordovician conodont fauna from the Mountain diatreme, northern Mackenzie Mountains, District of Mackenzie; Geological Survey of Canada, Paper 80–1A, p. 363–368. https://doi.org/10.4095/106226

Morrow, D.W., 1991. The Silurian-Devonian sequence in the northern part of the Mackenzie shelf, Northwest Territories; Geological Survey of Canada, Bulletin 413, 121 p. https://doi.org/10.4095/132170

Mortensen, J.K. and Card, K.D., 1993. U-Pb age constraints for the magmatic and tectonic evolution of the Pontiac Subprovince, Quebec; Canadian Journal of Earth Sciences, v. 30, p. 1970–1980. https://doi.org/10.1139/e93-173

Müller, W., Shelley, M., Miller, P., and Broude, S., 2009. Initial performance metrics of a new custom-designed AfF Excimer LA-ICP-MS system coupled to a two-volume laser-ablation cell; Journal of Analytical Atomic Spectrometry, v. 24, p. 209–214. https://doi.org/10.1039/B805995K

Norford, B.S. and Cecile, M.P., 1994. Ordovician emplacement of the Mount Dingley diatreme, western ranges of the Rocky Mountains, southeastern British Columbia; Canadian Journal of Earth Sciences, v. 31, p. 1491–1500. https://doi.org/10.1139/e94-132

Paces, J.B. and Miller, J.D., 1993. Precise U-Pb ages of Duluth Complex and related mafic intrusions, northeastern Minnesota: geochronological insights to physical, petrogenetic, paleomagnetic, and tectonomagmatic processes associated with the 1.1 Ga Midcontinent Rift System; Journal of Geophysical Research, v. 98, p. 13997–14013. https://doi.org/10.1029/93JB01159

Paton, C., Woodhead, J.D., Hellstrom, J.C., Hergt, J.M., Greig, A., and Maas, R., 2010. Improved laser ablation U-Pb zircon geochronology through robust downhole fractionation correction; Geochemistry Geophysics Geosystems, v. 11, p. 1–36. https://doi.org/10.1029/2009GC002618

Petrus, J.A. and Kamber, B.S., 2012. VizualAge: A novel approach to laser ablation ICP-MS U-Pb geochronology data reduction; Geostandards and Geoanalytical Research, v. 36, p. 247–270. https://doi.org/10.1111/j.1751-908X.2012.00158.x

Rainbird, R.H., Rayner, N.M., Hadlari, T., Heaman, L.M., Ielpi, A., Turner, E.C., and MacNaughton, R.B., 2017. Zircon provenance data record the lateral extent of pancontinental, Early Neoproterozoic rivers and erosional unroofing history of the Grenville orogeny; Geological Society of America Bulletin, v. 129, p. 1408–1423. https://doi.org/10.1130/B31695.1

Saylor, J.E. and Sundell, K.E., 2016. Quantifying comparison of large detrital geochronology data sets; Geosphere, v. 12, p. 203–220. https://doi.org/10.1130/GES01237.1

Spencer, C.J., Kirkland, C.L., and Taylor, R.J.M., 2016. Strategies towards statistically robust interpretations of in situ U-Pb zircon geochronology; Geoscience Frontiers, v. 7, p. 581–589. https://doi.org/10.1016/j.gsf.2015.11.006

Taylor, G.C., Campbell, R.B., and Norford, B.S., 1972. Silurian igneous rocks in the western Rocky Mountains, northeastern British Columbia; Geological Survey of Canada, Paper 72–1A, p. 228–229 https://doi.org/10.4095/119839

Vermeesch, P., 2018. IsoplotR: A free and open toolbox for geochronology; Geoscience Frontiers, v. 9, p. 1479–1493. https://doi.org/10.1016/j.gsf.2018.04.001

Wiedenbeck, M., Alle, P., Corfu, F., Griffin, W.L., Meier, M., Oberli, F., Von Quadt, A., Roddick, J.C., and Spiegel, W., 1995. Three natural zircon standards for U-Th-Pb, Lu-Hf, trace element and REE analysis; Geostandards Newsletter, v. 19, p. 1–23. https://doi.org/10.1111/j.1751-908X.1995.tb00147.x

Wiedenbeck, M., Hanchar, J.M., Peck, W.H., Sylvester, P., Valley, J., Whitehouse, M., Kronz, A., Morishita, Y., Nasdala, L., Fiebig, J., Franchi, I., Girard, J.P., Greenwood, R.C., Hinton, R., Kita, N., Mason, P.R.D., Norman, M., Ogasawara, M., Piccoli, P.M., Rhede, D., Satoh, H., Schulz-Dobrick, B., Skår, Ø., Spicuzza, M.J., Terada, K., Tindle, A., Togashi, S., Vennemann, T., Xie, Q., and Zheng, Y.F., 2004. Further characterisation of the 91500 zircon crystal; Geostandards and Geoanalytical Research, v. 28, p. 9–39. https://doi.org/10.1111/j.1751-908X.2004.tb01041.x